

Asymptotic dynamics of high dynamic range stratified turbulence

G. D. Portwood^{1,2}, S. M. de Bruyn Kops¹, and C. P. Caulfield^{3,4}

¹ *Department of Mechanical and Industrial Engineering,
University of Massachusetts, Amherst, USA 01003*

² *Methods and Algorithms (XCP-4), Computational Physics Division,
Los Alamos National Laboratory, Los Alamos, USA 87545*

³ *BP Institute, University of Cambridge, Cambridge, CB3 0EZ, UK and*

⁴ *Department of Applied Mathematics & Theoretical Physics,
University of Cambridge, Cambridge, CB3 0WA, UK*

(Dated: March 2, 2022)

Direct numerical simulations of homogeneous sheared and stably stratified turbulence are considered to probe the asymptotic high-dynamic range regime suggested by Gargett *et al.* [1] and Shih *et al.* [2]. We consider statistically stationary configurations of the flow that span three decades in dynamic range defined by the separation between the Ozmidov length scale, $L_O = \sqrt{\epsilon/N^3}$, and the Kolmogorov length scale, $L_K = (\nu^3/\epsilon)^{1/4}$, up to $\text{Re}_b \equiv (L_O/L_K)^{4/3} = \epsilon/(\nu N^2) \sim O(1000)$, where ϵ is the mean turbulent kinetic energy dissipation rate, ν is the kinematic viscosity, and N is the buoyancy frequency. We isolate the effects of Re_b , particularly on irreversible mixing, from the effects of other flow parameters of stratified and sheared turbulence [3]. Specifically, we evaluate the influence of dynamic range independent of initial conditions. We present evidence that the flow approaches an asymptotic state for $\text{Re}_b \gtrsim 300$, characterized both by an asymptotic partitioning between the potential and kinetic energies and by the approach of components of the dissipation rate to their expected values under the assumption of isotropy. As Re_b increases above 100, there is a slight decrease in the turbulent flux coefficient $\Gamma = \chi/\epsilon$, where χ is the dissipation rate of buoyancy variance, but, for this flow, there is no evidence of the commonly suggested $\Gamma \propto \text{Re}_b^{-1/2}$ dependence when $100 \leq \text{Re}_b \leq 1000$.

INTRODUCTION

Sheared, stratified turbulence, energized by vertical shearing of horizontal motions in the presence of a statically stable density distribution, arises throughout the world's oceans and atmosphere. Dynamical models of such flows, in particular capturing the vertical transport of heat due to irreversible mixing, are essential for modeling the global climate system because mixing occurs on relatively small scales, several orders of magnitude below those currently resolved in basin-scale models [4–6].

A key challenge for theoreticians is to develop a robust parameterization usable in such models for the vertical eddy diffusivity of heat κ_T defined as

$$\kappa_T \equiv \frac{B}{N^2} \equiv \frac{\langle \frac{g}{\rho_0} w \rho \rangle}{N^2}, \quad N \equiv \sqrt{-\frac{g}{\rho_0} \frac{d\bar{\rho}}{dz}}, \quad (1)$$

where angled brackets denote ensemble averaging, B is the buoyancy flux, N is the buoyancy frequency, g is the constant gravitational acceleration, ρ_0 is a constant reference density, (u, v, w) and ρ are the fluctuating velocity vector and fluctuating density, respectively, in the (x, y, z) coordinate system, and $\bar{\rho}$ is the mean ambient density with linear functional dependence in z . Here the Boussinesq approximation has been made such that density variations are sufficiently small so that a linear equation of state is appropriate and density variations are only significant in the buoyancy force.

Developing dynamical models of these complex flows has proved exceptionally difficult and controversial due

not least to their potential dependence on a wide range of parameters [3, 7]. For simplicity, we fix $\text{Pr} = \nu/\kappa = 1$, where ν is the kinematic viscosity and κ is the molecular thermal diffusivity. Even with this assumption, stratified sheared turbulence is influenced by at least four independent length scales, associated with characteristic values of overall stratification, shear and both the intensity and decay rate of turbulence [3]. The Ozmidov scale L_O , the Corrsin (or shear) scale L_C , the ‘large-eddy’ turbulent length scale L_L , and the Kolmogorov microscale L_K are defined here as

$$\begin{aligned} L_O &\equiv \left(\frac{\epsilon}{N^3}\right)^{1/2}; & L_C &\equiv \left(\frac{\epsilon}{S^3}\right)^{1/2}; \\ L_L &\equiv \frac{E_k^{3/2}}{\epsilon}; & L_K &\equiv \left(\frac{\nu^3}{\epsilon}\right)^{1/4}, \end{aligned} \quad (2)$$

where E_k is the averaged turbulent kinetic energy, ϵ is its dissipation rate and S is the mean constant vertical shear, i.e. $S \equiv d\bar{u}/dz$ where \bar{u} is the mean streamwise velocity with linear functional dependence in z . These four scales are determined by the properties of the fluctuation velocity field (i.e. the turbulence) relative to the background buoyancy frequency and shear. As noted by Ivey *et al.* [7], it is entirely plausible that length scales comparing the perturbation scalar field to these background quantities may be more physically relevant, although particularly in such stationary flows such as those considered here, it is entirely plausible that the various length scales may become closely coupled (as we investigate further below).

Although in general the scales defined in (2) vary in space and time [see e.g. 8], even in statistically stationary flows where characteristic values of these four length scales can be identified, parameterization of key properties of the flow could depend on at least three independent nondimensional parameters determined from these scales. Choices for these parameters are a characteristic Richardson number, Ri , a turbulent Froude number Fr and the activity parameter Re_b (sometimes called the buoyancy Reynolds number and formally distinct from a related integral-scale quantity; see Portwood *et al.* [9] for further discussion) defined as

$$Ri \equiv \frac{N^2}{S^2} \equiv \left(\frac{L_C}{L_O}\right)^{4/3},$$

$$Fr \equiv \frac{\epsilon}{NE_k} \equiv \left(\frac{L_O}{L_L}\right)^{2/3}, Re_b \equiv \frac{\epsilon}{\nu N^2} \equiv \left(\frac{L_O}{L_K}\right)^{4/3}, \quad (3)$$

although alternative parameters can be defined, such as a ‘shear number’ $S^* \equiv (L_L/L_C)^{2/3} \equiv SE_k/\epsilon \equiv 1/(Fr Ri^{1/2})$ and others [3].

In terms of these parameters, the central challenge regarding κ_T becomes that of determining the functional dependence of $\kappa_T(Ri, Fr, Re_b)$. In a profoundly influential paper, Osborn [10] argued from consideration of the turbulent kinetic energy equation that in stationary flows it is reasonable to suppose that the buoyancy flux B , or equivalently, for the stationary flows considered here, the dissipation rate of buoyancy variance χ defined as

$$\chi \equiv \kappa \left\langle \frac{g^2}{\rho_0^2 N^2} |\nabla \rho|^2 \right\rangle, \quad (4)$$

can be linearly related to the dissipation rate ϵ through a ‘turbulent flux coefficient’ or ‘mixing efficiency’ Γ , i.e. $\chi = \Gamma \epsilon$. Osborn hypothesized an upper bound for $\Gamma \leq 0.2$ on semi-empirical grounds, although in practice, Γ is implemented as a constant saturating the upper bound [6]. The introduction of Γ transforms the fundamental issue of modeling κ_T into identifying the functional dependence of $\Gamma(Ri, Fr, Re_b)$, since $\kappa_T = \nu \Gamma Re_b$ provided the flow is statistically stationary.

Many models have been presented for the functional dependence of Γ based on observations, experiments and numerical simulations in a variety of different flows, with much recent activity [e.g. 2, 4, 6, 11–18] though with little sign of consensus, due principally to three fundamental issues. Issue *I* is that disentangling transient and/or reversible processes from the irreversible processes crucial for quantifying and parameterizing mixing is extremely challenging. Issue *II* is that, even for flows where the assumption of stationarity is appropriate, stratification in a gravitational field and vertical shear both break isotropy, and so the extent to which anisotropy is important is difficult to determine, particularly when there is a relatively small dynamic range between L_K and $\min(L_C, L_O)$

(as encountered by Gargett *et al.* [1]). The condition $L_C < L_O$ is associated with growing and stationary flow configurations, as necessarily $Ri < 1$, suggesting that shear instabilities have to be sufficiently vigorous to sustain turbulence. This has the consequence that $L_C \gg L_K$ is a typical condition for high dynamic range, i.e. $Ri Re_b \gg 1$ by the relations defined in (3) and as suggested by Itsweire *et al.* [19]. Finally, issue *III* is that although in principle Re_b , Ri and Fr are all independent parameters, there is emerging evidence [e.g. 20] that in many flows the parameters become correlated, and so an apparent dependency of κ_T or Γ on one parameter is actually associated with variation in another parameter.

To address all three issues, we consider the model flow of *stationary homogeneous sheared and stratified turbulence* (S-HSST) [e.g. 2, 19, 21, 22]. In S-HSST, the production of turbulent kinetic energy by uniform mean vertical shear exactly balances the dissipation rates of kinetic and potential energy by molecular motion, addressing issue *I* by ensuring energetic stationarity by design. When numerically simulated, the turbulence fills the flow domain provided that Re_b is sufficiently large [23]. More generally, stratified turbulence has been shown to exhibit different dynamics depending on the value of Re_b [2, 24–27]. Gargett *et al.* [1] observed in limited two-point statistics from ocean data that Kolmogorov-Obukhov-Corrsin (KOC) scaling may be observed in stratified turbulence when $Re_b \sim O(10^3)$ and higher. de Bruyn Kops [26] observes that KOC scaling is generally not observed in DNS up to $Re_b = 220$, though some statistics may be consistent with such scalings. An important open question is thus how stratified turbulence behaves when $Re_b > O(100)$, a parameter space accessible by modern simulations of S-HSST with sufficiently small Fr for the stratification to have a first-order effect on the turbulent dynamics. However, to address issue *II* there is the further constraint that $Ri Re_b \gg 1$.

In fact, in S-HSST Ri and Fr cease to be free, but rather must adjust to ensure statistical stationarity. It has been empirically observed in simulations that the various dynamic length scales ‘tune’ so that $Fr \approx 0.5$ and $Ri \approx 0.16$, and equivalently $S^* \approx 5$. An immediate consequence of the emergence of an apparently Re_b -invariant stationary value of Ri in S-HSST is that issue *II* can indeed be addressed at sufficiently large Re_b .

Perhaps more importantly, issue *III* is also addressed, as the dependence of flow properties on Re_b can be probed independently of the other parameters. Specifically, although the adjustment of $Fr \approx 0.5$ and $Ri \approx 0.16$ occurs at $Re_b \sim O(10)$, other dynamical scalings have been observed to change as Re_b increases beyond $Re_b \sim O(100)$ [2, 26]. The objective of this study is thus to investigate how the key properties of the turbulence, in particular the energy partitioning, mixing and small-scale anisotropy depend on variations of Re_b . A specific question to investigate is whether the postulated

power law $\Gamma \propto \text{Re}_b^{-1/2}$ [2, 4, 18] for sufficiently large Re_b occurs in this flow in which dependence on other flow parameters can be completely eliminated.

SIMULATIONS

The incompressible Navier-Stokes equations are considered, subject to the nonhydrostatic Boussinesq approximation and coupled with equations for continuity and buoyancy transport. A turbulent decomposition is performed relative to a mean buoyancy gradient and a mean streamwise velocity gradient, both in the vertical direction [see also 21, 22, 28, 29]. We implement the system with the same Fourier pseudo-spectral scheme described by [26, 30], except that an additional shear term is handled by an integration factor [31–33].

Stationarity is induced by fixing a value of ν , choosing a target turbulent kinetic energy E_t then adjusting the Richardson number via g [c.f. 34] using a mass-spring-damper control system:

$$c_0 S \text{Ri}'(t) + 2\alpha\omega \tilde{E}_k'(t) + \omega^2(\tilde{E}_k(t) - 1) = 0 \quad (5)$$

where the prime notation denotes a temporal derivative, $\tilde{E}_k(t) \equiv E_k/E_t$ is the normalized turbulent kinetic energy, ω is the characteristic frequency of oscillation and α is a dimensionless damping factor. The control system has been derived by assuming that the kinetic energy follows a second order linear system [e.g. 35], and then by applying the first-order approximation $\tilde{E}_k'(t) \approx c_0 S(\text{Ri}(t) - \text{Ri}_c)$ such that $\tilde{E}_k''(t) \approx c_0 S \text{Ri}'(t)$. The parameter $c_0 \approx -1$ is supported by Jacobitz *et al.* [22], the characteristic frequency ω is determined by the mean shear, and a damping coefficient $\alpha = 1.5$ was found to work well.

Crucially, following this procedure, $\text{Ri} \approx 0.16$ emerges without presupposition for all our cases, as shown in the table I along with other emergent parameters; flow statistics are averaged over a period of $St \approx 100$ unless noted otherwise. Furthermore, the dissipation rate ϵ also ‘tunes’ such that $\text{Fr} \approx 0.5$. As the dissipation rate is an emergent quantity, the smallest length scales are resolved by adjusting the resolution such that $k_{max} L_K \approx 2$, where k_{max} is the largest Fourier domain wavenumber. We also found it necessary to use a relatively large domain with $L_x/L_y = 2$, $L_x/L_z = 4$ and $L_x/L_L \approx 40$, where L_x , L_y , and L_z are the dimensions of the domain, in order to support the anisotropic large scales of the flow.

RESULTS AND DISCUSSION

Energetics

We stress that, although $E_k \approx E_t$ is enforced, the parameters Ri , Fr and Re_b emerge from the simulations, as

Case	Re_b	Ri	Fr	N_x
SHSST-R1	36	0.163	0.46	1024
R2	48	0.159	0.47	1280
R3	59	0.162	0.48	1536
R4	81	0.154	0.50	1792
R5	110	0.155	0.52	2048
R6	160	0.157	0.48	3072
R7	240	0.156	0.48	4096
R8	390	0.146	0.46	6144
R9	550	0.163	0.45	8192
R10	900	0.152	0.42	9600

TABLE I. Simulation parameters. N_x is the number of grid points in the x -direction and the grid spacing is isotropic.

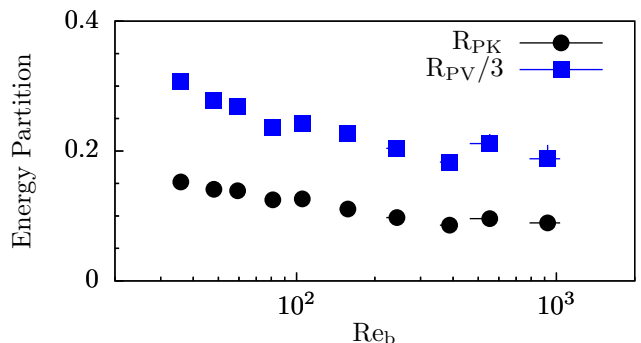


FIG. 1. Energy partitions as a function of Re_b . Bars indicate upper and lower quartile measurements of instantaneous quantities.

do the structure of the turbulence and the scalar. We consider the ratio of the potential energy to kinetic energy, $\text{R}_{PK} \equiv E_p/E_k$, and the ratio of the potential energy to the kinetic energy of vertical motion, $\text{R}_{PV} \equiv E_p/E_v$ where the energies are defined as:

$$E_v \equiv \frac{1}{2} \langle w^2 \rangle \text{ and } E_p \equiv \frac{1}{2} \left\langle \frac{g^2/\rho_0^2}{N^2} \rho^2 \right\rangle.$$

Energy-partitioning is a critical component to mixing models wherein Reynolds number, or Re_b , dependence is often omitted and the mixing is assumed to be a function of Ri [36–38]. Furthermore, in ‘strongly’ stratified turbulent flow, Billant and Chomaz [39] suggest that there should be approximate equipartition between potential and kinetic energy, i.e. $\text{R}_{PK} \approx 1$, an assumption also used by Lindborg [40]. Figure 1 illustrates that this basic assumption of equipartition is not appropriate. Perhaps more interesting, the energy ratios decrease by a factor of two relative to the lowest Re_b case until $\text{Re}_b \approx 300$, after which the energy ratios appear to remain constant with anisotropy of velocity variance explaining the different behaviors of R_{PK} and R_{PV} .

Small-scale anisotropy

The observation of anisotropy in the energy partitions of the previous section is particularly important, due not least to the inevitable requirement to estimate energetic dissipation rates in circumstances where each component of the rate-of-deformation tensor is not available. The existence of anisotropy at dissipative length scales would require dynamical estimates of κ_T to account for anisotropy. Therefore, it is necessary to evaluate common dissipation surrogate models to assess their applicability and to characterize small-scale anisotropy in these flows. Here, we use single component surrogate models which rely on a single derivative and the isotropy assumption:

$$\tilde{\epsilon}_{ij} = \begin{cases} 15\nu \left\langle \left(\frac{\partial u_i}{\partial x_j} \right)^2 \right\rangle & \text{if } i = j \\ 15/2\nu \left\langle \left(\frac{\partial u_i}{\partial x_j} \right)^2 \right\rangle & \text{if } i \neq j \end{cases} \quad (6a)$$

$$\tilde{\chi}_j = 3\kappa \left\langle \frac{g^2}{\rho_0^2 N^2} \left(\frac{\partial \rho}{\partial x_j} \right)^2 \right\rangle. \quad (6b)$$

In flows that are inherently anisotropic due to mean shear or mean flux, it is widely assumed that small-scale isotropy is a reasonable assumption when the scale separation is large [e.g. 1]. However, evidence suggests that isotropy assumptions can be very inaccurate in stably stratified flows at finite Re_b [19, 24, 26, 27].

The validity of (6) is tested with the help of figure 2 in which is plotted the relative error $(\tilde{\epsilon}_{ij} - \epsilon)/\epsilon$ of the various single-component dissipation estimates. As with energy partition, there is an apparently asymptotic regime for $Re_b \gtrsim 300$ in which the assumption of isotropy applied to dissipation rate becomes valid within approximately 15% error. Nevertheless, there is evidence of small-scale anisotropy as expected from the analysis in Durbin and Speziale [41], which shows that dissipation-range isotropy should only exist when $S^* \ll 1$; in these simulated flows $S^* \approx 5$. However, we observe that $\tilde{\epsilon}_{22}$, $\tilde{\epsilon}_{33}$, and $\tilde{\chi}_2$ yield good estimates of the dissipation rates even in cases in which the small scales are strongly anisotropic.

Mixing coefficient

We plot the turbulent mixing coefficient $\Gamma \equiv \chi/\epsilon$ in figure 3a. Whereas there is some modest decrease with increasing Re_b from the peak Γ of approximately 0.19, remarkably close to Osborn's suggested upper bound, there is no evidence of the commonly-suggested $Re_b^{-1/2}$ scaling [e.g. 2, 4, 18]. A decrease in mixing efficiency with respect to Re_b is observed until $Re_b \approx 200$, above which $\Gamma \approx 0.17$. There is no evidence of the 'energetic' regime of Shih *et al.* [2] for $Re_b > 100$, suggesting that transient multi-parameter effects may well be relevant in the evolution of their flows such that Re_b is not always an independent parameter (see issue III as described in §1). There

is evidence that the upper bound proposed by Osborn is a useful estimate, at least in flows where the underlying assumption of stationarity is well-justified, as such flows naturally adjust to $Ri \approx 0.16$ and $Fr \approx 0.5$.

Alternative descriptions of the mixing behavior are instructive. In the asymptotically high Re_b regime, the buoyancy variance dissipation rate adjusts such that $\chi \approx E_p N$ as evidenced by figures 1 and 3. Although this is a natural scaling, it is of interest that the $O(1)$ constant is actually extremely close to 1. A second instructive description of mixing is the turbulent Prandtl number $Pr_T = \kappa_M/\kappa_T$, where κ_M is the eddy diffusivity of momentum:

$$\kappa_M \equiv \frac{\langle uw \rangle}{S} = \frac{P}{S^2}, \quad (7)$$

and P is the production rate of turbulent kinetic energy. Therefore,

$$Pr_T = \frac{N^2}{S^2} \frac{P}{B} \equiv \frac{Ri}{Rf} \approx \frac{Ri(1+\Gamma)}{\Gamma}, \quad (8)$$

where Rf is the 'flux Richardson number', and the relationships $P \approx B + \epsilon = \chi + \epsilon$ in a stationary flow has been used. Pr_T is plotted in 3b, and proves to be close to one for all values of Re_b . This is perhaps unsurprising, but makes clear that the turbulent processes that mix heat and momentum in these flows are highly coupled, and in particular that the stratification is not sufficiently 'strong' to modify the turbulent processes greatly, but rather that the irreversible conversion of kinetic into potential energy occurs in a balanced, equilibrated way.

Using mixing length arguments, Odier *et al.* [42] defined:

$$L_\rho \equiv \left(\frac{B}{N^2 S} \right)^{1/2}; \quad L_m \equiv \left(\frac{P}{S^3} \right)^{1/2}; \quad (9)$$

such that $L_m^2/L_\rho^2 = Pr_T$. Therefore, since for our flows $Pr_T \approx 1$ and $P \approx (1+\Gamma)\epsilon$, it is apparent that the density length scale at the heart of the model presented by Ivey *et al.* [7] is coupled to the Corrsin scale by $L_\rho/L_C = \sqrt{1+\Gamma}$, and the key parameter $D \equiv \chi/\epsilon = 1/\Gamma$ has nearly fixed value.

CONCLUSIONS

We have used a canonical controlled flow to evaluate the isolated effects of high dynamic range in sheared stratified turbulent flow. The energy partitioning varies non-trivially where $Re_b \lesssim 300$ above which an apparently asymptotic regime is entered, consistent with [1, 26]. The flow retains measurable anisotropy at dissipation scales, as suggested by the analyses of Durbin and Speziale [41], at all values of Re_b we have considered. Nevertheless, some single-component surrogates exist which accurately

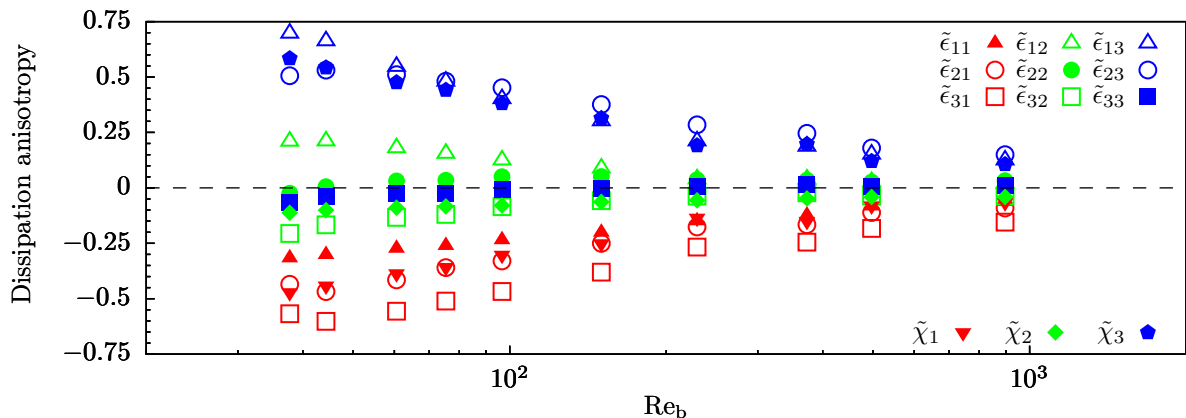


FIG. 2. Instantaneous measurements of small-scale anisotropy. The dashed line represents perfect isotropy at small scales.

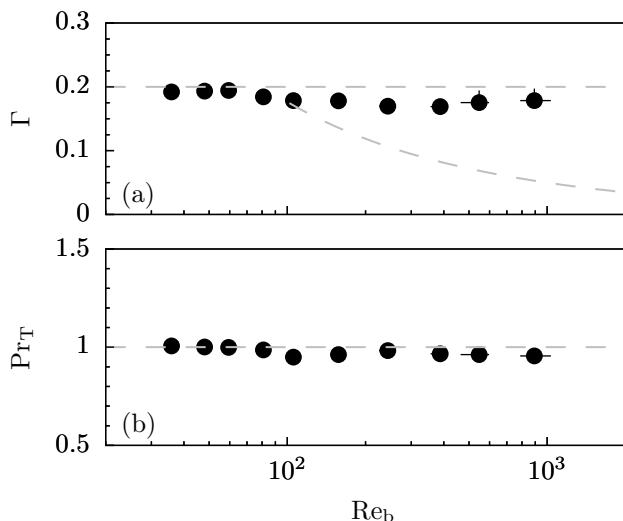


FIG. 3. a: Variation of turbulent flux coefficient Γ with Re_b . The upper bound proposed by Osborn is indicated by the gray dashed line where $\Gamma \approx 0.2$, and the $Re_b^{-1/2}$ -based parameterization suggested in Shih *et al.* [2] is plotted for their ‘energetic’ regime of $Re_b > 100$. b: Variation of turbulent Prandtl number Pr_T with Re_b .

estimate dissipation rates via isotropy assumptions even for smaller Re_b .

The results presented here seem to indicate that the effects of the large dynamic-range regimes explored by Gargett *et al.* are strongly influenced by asymptotic scalar density dynamics, rather than by the velocity field independently. Nevertheless, the measured mixing is a much weaker function of Re_b compared to some proposed scalings [2], with the turbulent Prandtl number $Pr_T \approx 1$ and the turbulent mixing coefficient Γ near the classical bound of 0.2 as suggested by Osborn, although decreasing slightly for $Re_b \lesssim 300$. The application of these results to higher Prandtl numbers merits further study, where dynamic range arguments indicate transition at lower Re_b

as Pr is increased.

We stress that the flow we have considered has, by design, controlled dependence on all other parameters. $Ri \approx 0.16$ and $Fr \approx 0.5$ naturally emerge to ensure stationarity. Therefore, we conjecture that observed apparent variation of mixing properties with Re_b [18] can be explained by breaking one or the other of these constraints, i.e. the variation is due to either transient effects, well-known to lead to strong variation in mixing properties [e.g 43, 44], or ‘hidden’ and perhaps correlated variation with other parameters [e.g 17]. Additionally, there could also be as yet unquantified strong dependence on initial or boundary conditions, whereas the flow we have considered is isolated from such effects. To develop robust mixing parameterizations, it is necessary to develop appropriate models to capture the effects of such conditions, informed by and generalizing from such controlled, idealized flows as considered here.

This work was funded by the U.S. Office of Naval Research via grant N00014-15-1-2248. High performance computing resources were provided through the U.S. Department of Defense High Performance Computing Modernization Program by the Army Engineer Research and Development Center, the Army Research Laboratory and the Navy DSRC under Frontier Project FP-CFD-FY14-007. The research activity of C.P.C. is supported by EPSRC Programme Grant EP/K034529/1 entitled ‘Mathematical Underpinnings of Stratified Turbulence’. Valuable comments from anonymous reviewers have substantially improved the clarity of the discussion.

-
- [1] A. Gargett, T. Osborn, and P. Nasmyth, *J. Fluid Mech.* **144**, 231 (1984).
 - [2] L. H. Shih, J. R. Koseff, G. N. Ivey, and J. H. Ferziger, *J. Fluid Mech.* **525**, 193 (2005).
 - [3] B. D. Mater and S. K. Venayagamoorthy,

- Phys. Fluids **26** (2014), 10.1063/1.4868142.
- [4] G. N. Ivey, K. B. Winters, and J. R. Koseff, *Annu. Rev. Fluid Mech.* **40**, 169 (2008).
 - [5] R. Ferrari and C. Wunsch, *Ann. Rev. Fluid Mech.* **41**, 253 (2009).
 - [6] M. C. Gregg, E. A. D’Asaro, J. J. Riley, and E. Kunze, *Ann. Rev. Mar. Sci.* **10**, 443 (2018).
 - [7] G. N. Ivey, C. E. Bluteau, and N. L. Jones, *J. Geophys. Res.-Oceans* **123**, 346 (2018).
 - [8] A. Mashayek, C. P. Caulfield, and W. R. Peltier, *J. Fluid Mech.* **736**, 570 (2013).
 - [9] G. D. Portwood, S. M. de Bruyn Kops, J. R. Taylor, H. Salehipour, and C. P. Caulfield, *J. Fluid Mech.* **807**, R2 (2016).
 - [10] T. R. Osborn, *J. Phys. Oceanogr.* **10**, 83 (1980).
 - [11] G. N. Ivey and J. Imberger, *J. Phys. Oceanogr.* **21**, 650 (1991).
 - [12] M. E. Barry, G. N. Ivey, K. B. Winters, and J. Imberger, *J. Fluid Mech.* **442**, 267 (2001).
 - [13] A. Maffioli, G. Brethouwer, and E. Lindborg, *J. Fluid Mech.* **794**, R3 (2016).
 - [14] A. Venaille, L. Gostiaux, and J. Sommeria, *J. Fluid Mech.* **810**, 554 (2017).
 - [15] H. Salehipour, W. R. Peltier, C. B. Whalen, and J. A. MacKinnon, *Geophys. Res. Lett.* **43**, 3370 (2016).
 - [16] A. Mashayek, H. Salehipour, D. Bouffard, C. P. Caulfield, R. Ferrari, M. Nikurashin, W. R. Peltier, and W. D. Smyth, *Geophys. Res. Lett.* **44**, 6296 (2017).
 - [17] Q. Zhou, J. R. Taylor, C. P. Caulfield, and P. F. Linden, *J. Fluid Mech.* **823**, 198 (2017).
 - [18] S. G. Monismith, J. R. Koseff, and B. L. White, *Geophys. Res. Lett.* **45**, 5627 (2018).
 - [19] E. C. Itsweire, J. R. Koseff, D. A. Briggs, and J. H. Ferziger, *J. Phys. Oceanogr.* **23**, 1508 (1993).
 - [20] D. Lucas and C. P. Caulfield, *J. Fluid Mech.* **832**, R1 (2017).
 - [21] S. E. Holt, J. R. Koseff, and J. H. Ferziger, *J. Fluid Mech.* **237**, 499 (1992).
 - [22] F. G. Jacobitz, S. Sarkar, and C. W. Van Atta, *J. Fluid Mech.* **342**, 231 (1997).
 - [23] D. C. Stillinger, K. N. Helland, and C. W. Van Atta, *J. Fluid Mech.* **131**, 91 (1983).
 - [24] D. A. Hebert and S. M. de Bruyn Kops, *Geophys. Res. Lett.* **33**, L06602 (2006).
 - [25] P. Bartello and S. M. Tobias, *J. Fluid Mech.* **725**, 1 (2013).
 - [26] S. M. de Bruyn Kops, *J. Fluid Mech.* **775**, 436 (2015).
 - [27] S. M. de Bruyn Kops and J. J. Riley, *J. Fluid Mech.* **860**, 787 (2019).
 - [28] R. S. Rogallo, *Numerical experiments in homogeneous turbulence*, Tech. Rep. TM-81315 (NASA, 1981).
 - [29] L. H. Shih, J. R. Koseff, J. H. Ferziger, and C. R. Rehmann, *J. Fluid Mech.* **412**, 1 (2000).
 - [30] S. Almalkie and S. M. de Bruyn Kops, *J. Turbul.* **13**, 1 (2012).
 - [31] K. A. Brucker, J. C. Isaza, T. Vaithianathan, and L. R. Collins, *J. Comp. Phys.* **225**, 20 (2007).
 - [32] D. Chung and G. Matheou, *J. Fluid Mech.* **696**, 434 (2012).
 - [33] A. Sekimoto, S. Dong, and J. Jiménez, *Phys. Fluids* **28**, 035101 (2016).
 - [34] J. R. Taylor, E. Deusebio, C. P. Caulfield, and R. R. Kerswell, *J. Fluid Mech.* **808**, R1 (2016).
 - [35] K. J. Rao and S. M. de Bruyn Kops, *Phys. Fluids* **23**, 065110 (2011).
 - [36] T. R. Osborn and C. S. Cox, *Geophysical & Astrophysical Fluid Dynamics* **3**, 321 (1972).
 - [37] U. Schumann and T. Gerz, *J. Appl. Meteorol.* **34**, 33 (1995).
 - [38] A. Pouquet, D. Rosenberg, R. Marino, and C. Herbert, *J. Fluid Mech.* **844**, 519 (2018).
 - [39] P. Billant and J.-M. Chomaz, *Phys. Fluids* **13**, 1645 (2001).
 - [40] E. Lindborg, *J. Fluid Mech.* **550**, 207 (2006).
 - [41] P. Durbin and C. Speziale, *J. Fluids Eng.* **113**, 707 (1991).
 - [42] P. Odier, J. Chen, M. K. Rivera, and R. E. Ecke, *prl* **102**, 134504 (2009).
 - [43] H. Salehipour, C. C. P., and W. Peltier, *J. Fluid Mech.* **803**, 591 (2016).
 - [44] A. Mashayek, C. P. Caulfield, and W. R. Peltier, *J. Fluid Mech.* **826**, 522 (2017).